

Simultaneous chromatic dispersion and PMD compensation by using coded-OFDM and girth-10 LDPC codes

Ivan B. Djordjevic, Lei Xu*, and Ting Wang*

University of Arizona, Department of Electrical and Computer Engineering, Tucson, AZ 85721, USA

*NEC Laboratories America, Princeton, NJ 08540, USA

ivan@ece.arizona.edu

Abstract: Low-density parity-check (LDPC)-coded orthogonal frequency division multiplexing (OFDM) is studied as an efficient coded modulation scheme suitable for simultaneous chromatic dispersion and polarization mode dispersion (PMD) compensation. We show that, for aggregate rate of 10 Gb/s, accumulated dispersion over 6500 km of SMF and differential group delay of 100 ps can be simultaneously compensated with penalty within 1.5 dB (with respect to the back-to-back configuration) when training sequence based channel estimation and girth-10 LDPC codes of rate 0.8 are employed.

©2008 Optical Society of America

OCIS codes: (060.4510) Optical communications; (999.9999) Polarization mode dispersion (PMD); (999.9999) Chromatic dispersion; (060.4080) Modulation; (060.4230) Multiplexing; (999.9999) Orthogonal frequency division multiplexing; (999.9999) Low-density parity-check (LDPC) codes

References and Links

1. R. Prasad, *OFDM for Wireless Communications Systems* (Artech House, Boston 2004).
2. I. B. Djordjevic and B. Vasic, "Orthogonal frequency-division multiplexing for high-speed optical transmission," *Opt. Express* **14**, 3767-3775 (2006).
3. W. Shieh and C. Athaudage, "Coherent optical frequency division multiplexing," *Electron. Lett.* **42**, 587-589 (2006).
4. A. J. Lowery, L. Du, and J. Armstrong, "Orthogonal frequency division multiplexing for adaptive dispersion compensation in long haul WDM systems," in *Proc. OFC Postdeadline Papers*, Paper no. PDP39, 2006.
5. I. B. Djordjevic and B. Vasic, "100 Gb/s transmission using orthogonal frequency-division multiplexing," *IEEE Photon. Technol. Lett.* **18**, 1576-1578 (2006).
6. I. B. Djordjevic, "PMD compensation in fiber-optic communication systems with direct detection using LDPC-coded OFDM," *Opt. Express* **15**, 3692-3701 (2007).
7. W. Shieh, "PMD-supported coherent optical OFDM systems," *IEEE Photon. Technol. Lett.* **19**, 134-136 (2006).
8. S. L. Jansen, I. Morita, N. Takeda, H. Tanaka, "20-Gb/s OFDM transmission over 4,160-km SSMF enabled by RF-pilot tone phase compensation," in *Proc. OFC/ NFOEC 2007 Postdeadline Papers*, Paper no. PDP15, March 25-29, 2007, Anaheim, CA, USA.
9. B. J. Schmidt, A. J. Lawery, J. Armstrong, "Experimental demonstration of 20 Gbit/s direct-detection optical OFDM and 12 Gbit/s with a colorless transmitter," in *Proc. OFC/ NFOEC 2007 Postdeadline Papers*, Paper no. PDP18, March 25-29, 2007, Anaheim, CA, USA.
10. A. Lowery, "Nonlinearity and its compensation in optical OFDM systems," presented at ECOC 2007 Workshop 5 (Electronic signal processing for transmission impairment mitigation: future challenges).
11. I. B. Djordjevic, H. G. Batshon, M. Cvijetic, L. Xu, and T. Wang, "PMD compensation by LDPC-coded turbo equalization," *IEEE Photon. Technol. Lett.* **19**, 1163 - 1165 (2007).
12. W. Shieh, X. Yi, Y. Ma, and Y. Tang, "Theoretical and experimental study on PMD-supported transmission using polarization diversity in coherent optical OFDM systems," *Opt. Express* **15**, 9936-9947 (2007).
13. I. B. Djordjevic, S. Sankaranarayanan, S. K. Chilappagari, and B. Vasic, "Low-density parity-check codes for 40 Gb/s optical transmission systems," *IEEE J. Sel. Top. Quantum Electron.* **12**, 555-562 (2006).
14. M. P. C. Fossorier, "Quasi-cyclic low-density parity-check codes from circulant permutation matrices," *IEEE Trans. Inform. Theory* **50**, 1788-1794 (2004).
15. O. Milenkovic, I. B. Djordjevic, and B. Vasic, "Block-circulant low-density parity-check codes for optical communication systems," *IEEE J. Sel. Top. Quantum Electron.* **10**, 294-299 (2004).

16. J. L. Fan, "Array codes as low-density parity-check codes," in Proc. 2nd Int. Symp. Turbo Codes and Related Topics, Brest, France, pp. 543-546, Sept. 2000.
 17. D. J. C. MacKay, "Good error correcting codes based on very sparse matrices," IEEE Trans. Inform. Theory **45**, 399-431 (1999).
 18. R. M. Tanner, "A recursive approach to low complexity codes," IEEE Trans. Inf. Theory **IT-27**, 533-547 (1981).
 19. T. Mizuochoi, Y. Miyata, T. Kobayashi, K. Ouchi, K. Kuno, K. Kubo, K. Shimizu, H. Tagami, H. Yoshida, H. Fujita, M. Akita, and K. Motoshima, "Forward error correction based on block turbo code with 3-bit soft decision for 10-Gb/s optical communication systems," IEEE J. Sel. Top. Quantum Electron. **10**, 376-386 (2004).
 20. N. Cvijetic, L. Xu, and T. Wang, "Adaptive PMD Compensation using OFDM in Long-Haul 10Gb/s DWDM Systems," in Optical Fiber Comm. Conf., Paper OTuA5, Anaheim, CA (2007).
-

1. Introduction

Orthogonal frequency division multiplexing (OFDM) [1-10] represents a particular multicarrier transmission scheme in which a single information-bearing stream is transmitted over many lower rate sub-channels. OFDM has already been considered for use in fiber-optics communication systems by numerous researchers [2-10]. Because the subcarriers in OFDM are orthogonal the partial overlap of neighboring frequency slots is allowed resulting in improved spectral efficiency as compared to a conventional multicarrier system. By using a sufficiently large number of sub-carriers and cyclic extension principle, the intersymbol interference (ISI) due to chromatic dispersion and polarization mode dispersion (PMD) can be significantly reduced [4-9]. To simultaneously compensate both residual chromatic dispersion and PMD someone may use the turbo equalization [11] or maximum-likelihood sequence detection (MLSD). However, the complexity of such an equalizer grows exponentially as accumulated chromatic dispersion and differential group delay increase. On the other hand, in OFDM, in order to improve the tolerance against chromatic dispersion and PMD someone needs to increase the guard interval only, which does not introduce any complexity compared to the turbo equalization or MLSD.

In most of the publications related to OFDM (see [2-10]), different channel impairments, such as chromatic dispersion, PMD, and intrachannel nonlinearities, were studied by observing scenarios in which each particular impairment dominates, although in practice those impairments act simultaneously. The recent reference [12], in which coherent OFDM transmission is observed, is an exception from this common practice. In this paper we show that LDPC-coded OFDM with direct detection is an excellent candidate for simultaneous chromatic dispersion and PMD compensation. Moreover, we propose a new class of LDPC codes suitable for use in coded-OFDM, which is based on *large girth* quasi-cyclic LDPC codes (the girth represents the shortest cycle in corresponding bipartite graph representation of a parity-check matrix). To facilitate the implementation at high-speed we prefer the use of structured LDPC codes [13-16] rather than random LDPC codes [17]. To reduce the performance loss of structured LDPC codes, compared to random ones, we use the girth as the optimization parameter, and design the LDPC codes of girth-10, as explained in Section 3. Notice that girth-10 LDPC codes significantly outperform the girth-6 LDPC codes we proposed in [6], and outperform the girth-8 LDPC codes by about 0.5 dB (see Section 3). Given the fact that length of girth-12 LDPC codes approaches 100000 of bits, the girth-10 LDPC codes seem to represent a reasonable FEC option for high-speed implementation.

Because the state-of-the-art fiber-optic communication systems essentially use the intensity modulation/direct detection (IM/DD), we consider the LDPC-coded optical OFDM communications with direct detection only. The coherent optical OFDM systems require the use of an additional local laser, which increases the receiver complexity, and are sensitive to the laser phase noise. In most of OFDM proposals for fiber-optics channels, both in-phase (I) and quadrature (Q) channels are to be transmitted (e.g., [3,4]). In our version of OFDM only the transmission of I-channel is sufficient. In what follows, we will show that by using coded-OFDM with training sequence based channel estimation, equipped with girth-10 LDPC codes, it is possible to simultaneously compensate for the accumulated chromatic dispersion over 6500 km of SMF and 100 ps of differential group delay with penalty (against the back-to-back

configuration) being less than 1.5 dB, in an optical transmission system of aggregate rate 10 Gb/s.

The paper is organized as follows. The concept of LDPC-coded OFDM transmission is introduced in Section 2. In Section 3 we describe a class of large-girth LDPC codes suitable for use in coded-OFDM. In Section 4 we provide the numerical results to illustrate the suitability of LDPC-coded OFDM in simultaneous chromatic dispersion and PMD compensation. Finally, in Section 5 some important concluding remarks are given.

2. LDPC-coded optical OFDM Transmission

The transmitter and receiver configurations are shown in Figs. 1(a), and 1(b), respectively. On the transmitter side the information-bearing streams at 10 Gb/s are encoded using identical LDPC codes. The outputs of these LDPC encoders are demultiplexed and parsed into groups of B_{tot} bits corresponding to one OFDM frame. The B_{tot} bits in each OFDM frame are subdivided into N_{QAM} sub-channels with the i^{th} sub-carrier carrying b_i bits, $B_{\text{tot}} = \sum_{i=1}^{N_{\text{QAM}}} b_i$.

The b_i bits from the i^{th} sub-channel are mapped into a complex-valued signal from a 2^{b_i} -point QAM signal constellation. For example, $b_i=2$ for QPSK and $b_i=4$ for 16-QAM. Notice that different sub-carriers may carry different number of bits. The complex-valued signal points from sub-channels are considered to be the values of the fast Fourier transform (FFT) of a multi-carrier OFDM signal. The OFDM symbol is generated as follows: N_{QAM} input QAM symbols are zero-padded to obtain N_{FFT} input samples for inverse FFT (IFFT), N_G non-zero samples are inserted to create the guard interval, and the OFDM symbol is multiplied by the window function. The purpose of cyclic extension is to preserve the orthogonality among sub-carriers when the neighboring OFDM symbols partially overlap due to chromatic dispersion and PMD, and the role of windowing is to reduce the out-of band spectrum. For efficient chromatic dispersion and PMD compensation, the length of cyclically extended guard interval should be smaller than the total spread due to chromatic dispersion and DGD. The cyclic extension is accomplished by repeating the last $N_G/2$ samples of the effective OFDM symbol part (N_{FFT} samples) as a prefix, and repeating the first $N_G/2$ samples as a suffix. After D/A conversion and RF up-conversion, the RF signal can be converted into the optical domain using one of two possible options: (i) the OFDM signal can directly modulate a distributed-feedback (DFB) laser, or (ii) the OFDM signal can be used as the RF input of a Mach-Zehnder modulator (MZM). A DC bias component is added to the OFDM signal in order to enable recovery of the QAM symbols using direct detection. Because bipolar signals cannot be transmitted over an IM/DD link, the bias component should be sufficiently large so that (when added to the OFDM signal) the resulting signal is non-negative. The main disadvantage of this approach scheme is the poor power efficiency. To improve the OFDM power efficiency two alternative schemes can be used: (i) the ‘‘clipped-OFDM’’ (C-OFDM) scheme, which is based on single-side band (SSB) transmission and clipping of the OFDM signal after the bias addition, and (ii) the ‘‘unclipped-OFDM’’ (U-OFDM) scheme, which is based on SSB transmission using a LiNbO₃ MZM. To avoid distortion due to clipping at the transmitter in the U-OFDM scheme, the information can be imposed by modulating the electrical field of the optical carrier. In this way both positive and negative portions of the electrical OFDM signal can be transmitted up to the photodetector. Distortion introduced by the photodetector, caused by squaring, can be successfully eliminated by proper filtering, as shown later in this Section. It is important to note, however, that the U-OFDM scheme is less power efficient than the C-OFDM scheme. The SSB modulation can be achieved either by appropriate optical filtering the double-side band signal at MZM output [see Fig. 1(a)] or by using the Hilbert transformation of in-phase component of OFDM RF signal. The first version requires the use of only in-phase component of RF OFDM signal, providing that zero-padding is done in the middle of OFDM symbol rather than at the edges. The transmitted OFDM signal is real and can be written as

$$s(t) = s_{\text{OFDM}}(t) + D, \quad (1)$$

where

$$s_{\text{OFDM}}(t) = \text{Re} \left\{ \sum_{k=-\infty}^{\infty} w(t-kT) \sum_{i=-N_{\text{FFT}}/2}^{N_{\text{FFT}}/2-1} X_{i,k} \cdot e^{j2\pi \frac{i}{T_{\text{FFT}}}(t-kT)} e^{j2\pi f_{\text{RF}} t} \right\}$$

is defined for $t \in [kT - T_G/2 - T_{\text{win}}, kT + T_{\text{FFT}} + T_G/2 + T_{\text{win}}]$. In the above expression $X_{i,k}$ denotes the i th subcarrier of the k th OFDM symbol, $w(t)$ is the window function, and f_{RF} is the RF carrier frequency. T denotes the duration of the OFDM symbol, T_{FFT} denotes the FFT sequence duration, T_G is the guard interval duration (the duration of cyclic extension), and T_{win} denotes the windowing interval duration. D denotes the DC bias component, which is introduced to enable the OFDM demodulation using the direct detection.

The PIN photodiode output current can be written as

$$i(t) = R_{\text{PIN}} \left\{ \left[s_{\text{OFDM}}(t) + D \right] * h(t) + N(t) \right\}^2, \quad (2)$$

where $s_{\text{OFDM}}(t)$ denotes the transmitted OFDM signal in RF domain given by (1). D is introduced above, while R_{PIN} denotes the photodiode responsivity. The impulse response of the optical channel is represented by $h(t)$, with operator $*$ being the convolution operator. The $N(t)$ represents the amplified spontaneous emission (ASE) noise. The signal after RF down-conversion and appropriate filtering, can be written as

$$r(t) = \left[i(t) k_{\text{RF}} \cos(\omega_{\text{RF}} t) \right] * h_e(t) + n(t), \quad (3)$$

where $h_e(t)$ is the impulse response of the low-pass filter, $n(t)$ is electronic noise in the receiver, and k_{RF} denotes the RF down-conversion coefficient. Finally, after the A/D conversion and cyclic extension removal, the signal is demodulated by using the FFT algorithm. The soft outputs of the FFT demodulator are used to estimate the bit reliabilities that are fed to identical LDPC iterative decoders implemented based on the sum-product algorithm [13].

For the sake of illustration, let us consider the signal waveforms and power-spectral densities (PSDs) at various points in the OFDM system given in Fig. 1. These examples are generated using SSB transmission in a back-to-back configuration. The bandwidth of the OFDM signal is set to B GHz, and the RF carrier to $0.75B$. With B we denoted the total symbol transmission rate. The number of OFDM sub-channels is set to 64, the OFDM sequence is zero-padded, and the FFT is calculated using 128 points. The guard interval is obtained by a cyclic extension of 2×16 samples. The average transmitted launch power, in this back-to-back example, is set to 0dBm. The OFDM transmitter parameters are carefully chosen such that RF driver amplifier and MZM, as shown in Figs. 2(a)-2(b), operate in the linear regime. The PSDs of MZM output signal, and the photodetector output signal are shown in Figs. 2(c) and 2(d), respectively. The OFDM term after beating in the photodetector (PD), the low-pass term, and the squared OFDM terms can easily be identified.

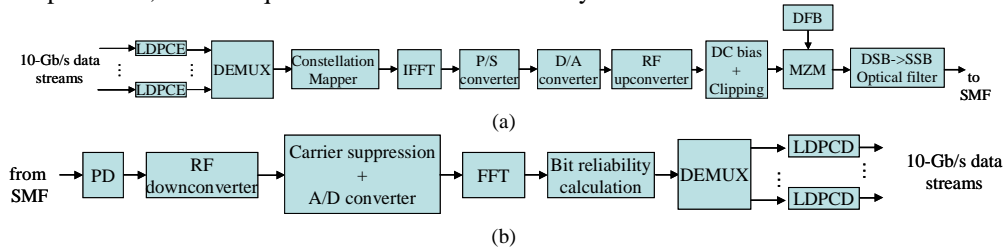


Fig. 1. LDPC-coded OFDM: (a) transmitter configuration, and (b) receiver configuration. LDPC-E-LDPC encoder, LDPC-D-LDPC decoder, S/P-serial-to-parallel converter, MZM-Mach-Zehnder modulator, SMF-single-mode optical fiber, PD-photodetector, DSB-double-sideband, SSB-single-sideband.

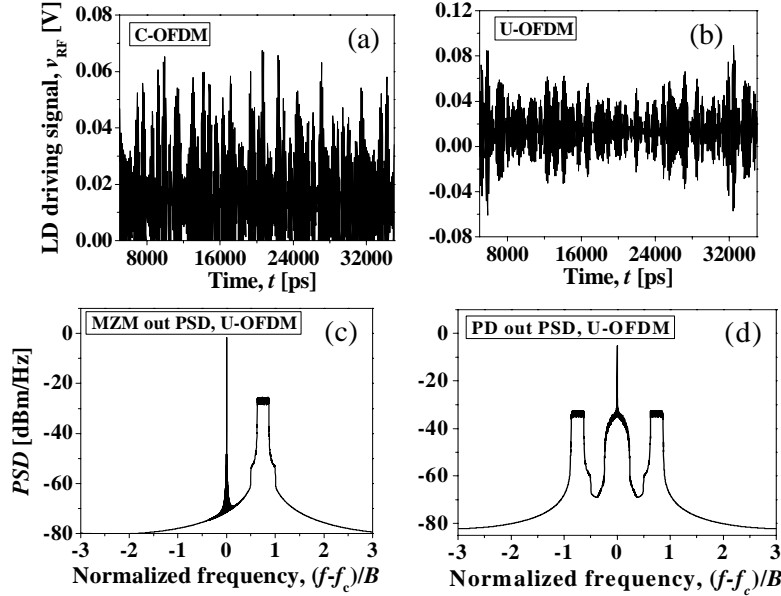


Fig. 2. Waveforms and PSDs of SSB QPSK-OFDM signal at different points during transmission for electrical SNR (per bit) of 6dB. (f_c denotes the optical carrier frequency, LD denotes the laser diode).

Notice that our proposal requires the use of only I-channel, while both the coherent detection version due to Shieh [3] and the direct detection version due to Lowery [4] require the use of I- and Q-channels. In our recent paper [6] we have shown that coded OFDM is an excellent candidate to be used in PMD compensation. In the same paper we designed the girth-6 LDPC codes suitable for use in PMD compensation by coded-OFDM, because they have small number of cycles of length 6. Moreover, the bit-error rate (BER) performance was evaluated observing the thermal noise dominated scenario. In next Section, we will describe the new class of quasi-cyclic LDPC codes suitable for use in coded-OFDM optical transmission, the girth-10 LDPC codes. Those codes, significantly outperform the girth-6 codes, and provide about 0.5 dB improvement in coding gain over girth-8 LDPC codes and about 1 dB improvement over turbo-product codes. Later, in Section 4, we study the efficiency of coded-OFDM based on girth-10 LDPC codes in simultaneous suppression of chromatic dispersion and PMD, observing the ASE noise dominated scenario.

3. Large girth block-circulant (array) LDPC codes

Now we turn our attention to the design of LDPC codes of large girth. Based on Tanner's bound for the minimum distance of an LDPC code [18]

$$d \geq \begin{cases} 1 + \frac{r}{r-2} \left((r-1)^{\lfloor (g-2)/4 \rfloor} - 1 \right), & g/2 = 2m+1 \\ 1 + \frac{r}{r-2} \left((r-1)^{\lfloor (g-2)/4 \rfloor} - 1 \right) + (r-1)^{\lfloor (g-2)/4 \rfloor}, & g/2 = 2m \end{cases} \quad (4)$$

where g and r denote the girth of the code graph and the column weight, respectively, and where d stands for the minimum distance of the code. It follows that large girth leads to an exponential increase in the minimum distance, providing that the column weight is at least 3. ($\lfloor \cdot \rfloor$ denotes the largest integer less than or equal to the enclosed quantity.) For example, the minimum distance of girth-10 codes with column weight $r=3$ is at least 10.

The structured LDPC codes introduced in this Section belong to the class of quasi-cyclic [14,15] or array [16] codes. Their parity-check matrix can be represented by

$$H = \begin{bmatrix} I & P^{c_0} & P^{2c_0} & \dots & P^{(q-1)c_0} \\ I & P^{c_1} & P^{2c_1} & \dots & P^{(q-1)c_1} \\ \dots & \dots & \dots & \dots & \dots \\ I & P^{c_{r-1}} & P^{2c_{r-1}} & \dots & P^{(q-1)c_{r-1}} \end{bmatrix}, \quad (5)$$

where $c_i \in \{0, 1, \dots, q-1\}$ ($i=0, 1, \dots, r-1$), I is the identity matrix of dimension q , and P denotes the permutation matrix

$$P = \begin{bmatrix} 0 & 1 & 0 & 0 & \dots & 0 \\ 0 & 0 & 1 & 0 & \dots & 0 \\ \dots & \dots & \dots & \dots & \dots & \dots \\ 0 & 0 & 0 & 0 & \dots & 1 \\ 1 & 0 & 0 & 0 & \dots & 0 \end{bmatrix}$$

The integers c_i are to be carefully chosen according to [14] in order to avoid the cycles of length $2k$ ($k=3$ or 4). According to [14] (see also [16]) the cycle of length $2k$ exists if we can find the closed path in (5), denoted by $(i_1, j_1), (i_1, j_2), (i_2, j_2), (i_2, j_3), \dots, (i_k, j_k), (i_k, j_1)$, such that

$$c_{i_1} j_1 + c_{i_2} j_2 + \dots + c_{i_k} j_k = c_{i_1} j_2 + c_{i_2} j_3 + \dots + c_{i_k} j_1 \pmod{q}, \quad (6)$$

where q is the dimension of the permutation matrix P , and must be a prime number. The pair of indices above denote row-column indices of permutation-blocks in (5) such that $l_m \neq l_{m+1}$, $l_k \neq l_1$ ($m=1, 2, \dots, k$; $l \in \{i, j\}$). In order to avoid the cycles of length $2k$, $k=3$ or 4 , we have to find the sequence of integers $c_i \in \{0, 1, \dots, q-1\}$ ($i=0, 1, \dots, r-1$; $r < q$) not satisfying the Eq. (6), which can be done either by computer search or in a combinatorial fashion. For example, to design the LDPC codes in [15] we introduced the concept of the cyclic-invariant difference set (CIDS). The CIDS-based codes come naturally as girth-6 codes, and to increase the girth we had to selectively remove certain elements from the CIDS. The design of LDPC codes of rate above 0.8, column weight 3 and girth-10 using the CIDS approach is a very challenging, and still an open problem. Instead, in this paper we solve this problem by developing an efficient computer search algorithm, which begins with an initial set S . We add an additional integer at a time from the set $Q = \{0, 1, \dots, q-1\}$ (not used before) to the initial set S and check if the Eq. (6) is satisfied. If the Eq. (6) is satisfied we remove that integer from the set S , and continue our search with another integer from set Q , until we exploit all the elements from Q . The code rate R is lower-bounded by

$$R \geq \frac{nq - rq}{nq} = 1 - r/n, \quad (7)$$

and the code length is nq , where n denotes the number of elements from S being used. The parameter n is determined by desired code rate R_0 by $n=r/(1-R_0)$. If desired code rate is set to $R_0=0.8$, and column weight to $r=3$, the parameter $n=5r$.

Example: By setting $q=1129$, the set of integers to be used in (5) is obtained as $S = \{0, 1, 4, 11, 27, 39, 48, 84, 134, 163, 223, 284, 333, 397, 927\}$. The corresponding LDPC code has rate $R_0=1-3/15=0.8$, column weight 3, girth-10 and length $nq=15 \cdot 1129=16935$, which is about twice shorter than turbo-product code (TPC) proposed in [19]. In the example above, the initial set of integers was $S=\{0, 1, 4\}$. The use of a different initial set will result in a different set from that obtained above. In addition to this code, we also designed the LDPC(24015, 19212) code of rate 0.8, girth-10 and column weight 3.

The results of simulations for an additive white Gaussian noise (AWGN) channel model are given in Fig. 3, where we compare the proposed LDPC codes against RS, concatenated RS, turbo-product, and girth-8 LDPC codes. The girth-10 LDPC(24015, 19212) code of rate 0.8 outperforms the concatenation RS(255, 239)+RS(255, 223) (of rate 0.82) by 3.35 dB, and RS(255, 239) by 4.75 dB, both at BER of 10^{-7} . At BER of 10^{-10} it outperforms lattice based

LDPC(8547,6922) of rate 0.81 and girth-8 by 0.44 dB, and BCH(128,113)xBCH(256,239) TPC of rate 0.82 by 0.95 dB. The net effective coding gain at BER of 10^{-12} is 10.95 dB, which represents the largest net effective coding gain, on an AWGN channel, ever reported in optical communications.

Given this description of LDPC-coded OFDM, and the design of LDPC codes to be used in coded-OFDM, in the following Section we describe our application of interest: the use of LDPC-coded OFDM in simultaneous chromatic dispersion and PMD compensation.

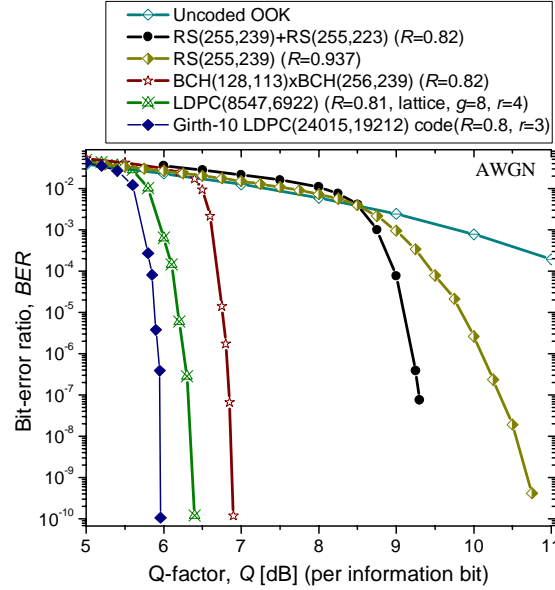


Fig. 3. The girth-10 LDPC code against RS, concatenated RS, turbo-product, and girth-8 LDPC codes on an AWGN channel model.

4. Simultaneous chromatic dispersion and PMD compensation via LDPC-coded OFDM

The receiver commonly employs the trans-impedance amplifier (TA) design, because it provides a good compromise between noise characteristics and supported bandwidth. The received electrical field, at the input of the TA, in the presence of chromatic dispersion and first-order PMD, can be represented by

$$E(t) = FT^{-1} \left\{ FT \left\{ E_0 \left[\begin{array}{c} \sqrt{1-\kappa} \\ \sqrt{\kappa} e^{j\delta} \end{array} \right] \left[S_{OFDM}(t) + b \right] \right\} e^{j \left(\frac{\beta_2 \omega^2}{2} - \frac{\beta_3 \omega^3}{6} \right) L_{tot}} \right\} + \begin{bmatrix} N_x(t) \\ N_y(t) \end{bmatrix}, \quad (8)$$

where β_2 and β_3 represent the group-velocity dispersion (GVD) and second order GVD parameters, L_{tot} is the total SMF length, k is the splitting ratio between two principle states of polarization (PSPs), δ is the phase difference between PSPs, E_0 is transmitted laser electrical field amplitude, and N_x and N_y represent x - and y -polarization ASE noise components. With FT and FT^{-1} we denoted the Fourier transform and inverse Fourier transform, respectively. The TA output signal can be represented by $v(t) = R_F R_{PIN} |E(t)|^2 + n(t)$, where R_{PIN} is the photodiode responsivity, R_F is the TA feedback resistor, and $n(t)$ is TA thermal noise. For complete elimination of ISI, the total delay spread due to chromatic dispersion and DGD should be smaller than the guard time:

$$\left| \beta_2 \right| L_{tot} \Delta\omega + DGD_{max} = \frac{c}{f^2} \left| D_t \right| N_{FFT} \Delta f + DGD_{max} \leq T_G, \quad (9)$$

where D_t is the accumulated dispersion, Δf is the sub-carrier spacing, c is the speed of the

light, and f is the central frequency set to 193.1 THz. The number of subcarriers N_{FFT} , the guard interval T_G , GVD and second-order GVD parameters were introduced earlier. The received QAM symbol of i -th subcarrier in the k -th OFDM symbol is related to transmitted QAM symbol $X_{i,k}$ by

$$Y_{i,k} = h_i e^{j\theta_i} e^{j\phi_k} X_{i,k} + n_{i,k}, \quad (10)$$

where h_i is channel distortion introduced by PMD and chromatic dispersion, and θ_i is the phase shift of i -th sub-carrier due to chromatic dispersion. ϕ_k represents the OFDM symbol phase noise due to SPM and RF down-converter, and can be eliminated by pilot-aided channel estimation. Notice that in direct detection case, the laser phase noise is completely cancelled by photodetection. To estimate the channel distortion due to PMD, h_i and phase shift due to chromatic dispersion θ_i , we need to pre-transmit the training sequence. Because in ASE noise dominated scenario (considered here) the channel estimates are sensitive to ASE noise, the training sequence should be sufficiently long to average the noise. For DGDs up to 100 ps, the training sequence composed of several OFDM symbols is sufficient. For larger DGDs longer OFDM training sequence is required; alternatively, the channel coefficients can be chosen to maximize the log-likelihood ratios (LLRs) or someone can use the polarization beam splitter to separate the x - and y -polarization components, and consequently process them. The phase shift of i th subcarrier due to chromatic dispersion can be determined from training sequence as difference of transmitted and received phase averaged over different OFDM symbols. Once the channel coefficients and phase shifts due to PMD and chromatic dispersion are determined, in a decision-directed mode, the transmitted QAM symbols are estimated by

$$\hat{X}_{i,k} = \left(h_i^* / |h_i|^2 \right) e^{-j\theta_i} e^{-j\phi_k} Y_{i,k}. \quad (11)$$

The symbol LLRs $\lambda(q)$ ($q=0,1,\dots,2^b-1$) can be determined by

$$\lambda(q) = -\frac{\left(\text{Re}[\hat{X}_{i,k}] - \text{Re}[\text{QAM}(\text{map}(q))] \right)^2}{N_0} - \frac{\left(\text{Im}[\hat{X}_{i,k}] - \text{Im}[\text{QAM}(\text{map}(q))] \right)^2}{N_0}; \quad q = 0, 1, \dots, 2^b - 1 \quad (12)$$

where $\text{Re}[\cdot]$ and $\text{Im}[\cdot]$ denote the real and imaginary part of a complex number, QAM denotes the QAM-constellation diagram, N_0 denotes the power-spectral density of an equivalent Gaussian noise process obtained from training sequence, and $\text{map}(q)$ denotes a corresponding mapping rule (Gray mapping is applied here). (b denotes the number of bits per constellation point.) Let us denote by v_j the j th bit in an observed symbol q binary representation $\mathbf{v}=(v_1, v_2, \dots, v_b)$. The bit LLRs needed for LDPC decoding are calculated from symbol LLRs by

$$L(\hat{v}_j) = \log \frac{\sum_{q:v_j=0} \exp[\lambda(q)]}{\sum_{q:v_j=1} \exp[\lambda(q)]}, \quad (13)$$

Therefore, the j th bit reliability is calculated as the logarithm of the ratio of a probability that $v_j=0$ and probability that $v_j=1$. In the nominator, the summation is done over all symbols q having 0 at the position j , while in the denominator over all symbols q having 1 at the position j .

The results of simulation, for ASE noise dominated scenario and single wavelength channel transmission, are shown in Figs. 4-6, for the LDPC-coded SSB OFDM system with aggregate rate of 10 Gb/s, 512 sub-carriers, RF carrier frequency of 10 GHz, oversampling factor of 2, and cyclic extension with 512 samples. The modulation format being applied is QPSK. The LDPC(16935,13550) code of girt-10, code rate 0.8, and column-weight 3, designed as explained in Section 3 is used. In Fig. 4 we show the BER performance for DGD of 100 ps, without residual chromatic dispersion. We see that uncoded case faces significant performance degradation at low BERs. On the other hand, the LDPC-coded case has

degradation of 1.1 dB at BER of 10^{-9} (when compared to the back-to-back configuration). In Fig. 5 we show the BER performance after 6500 km of SMF (without optical dispersion compensation), for a dispersion map composed of 65 sections of SMF with 100 km in length. The noise figure of erbium-doped fiber amplifiers (EDFAs), deployed periodically after every SMF section, was set to 5 dB. To achieve the desired OSNR, the ASE noise loading was applied on receiver side, while the launch power was kept below 0 dBm. We see that LDPC-coded OFDM is much less sensitive to chromatic dispersion compensation than PMD. Therefore, even 6500 km can be reached without optical dispersion compensation with penalty within 0.4 dB at BER of 10^{-9} , when LDPC-coded OFDM is used.

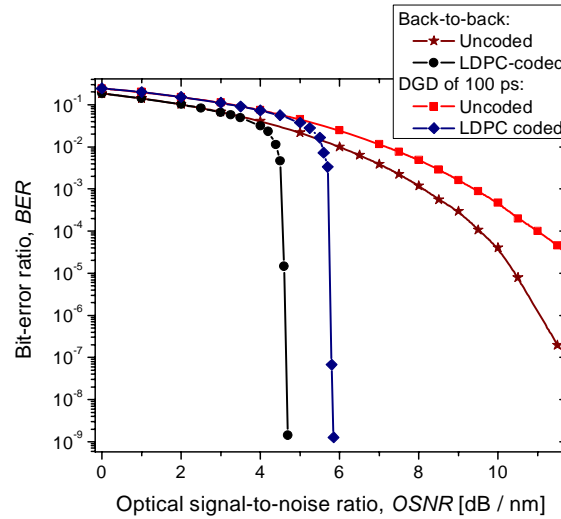


Fig. 4. BER performance of LDPC-coded OFDM system with aggregate rate of 10 Gb/s, for DGD of 100 ps.

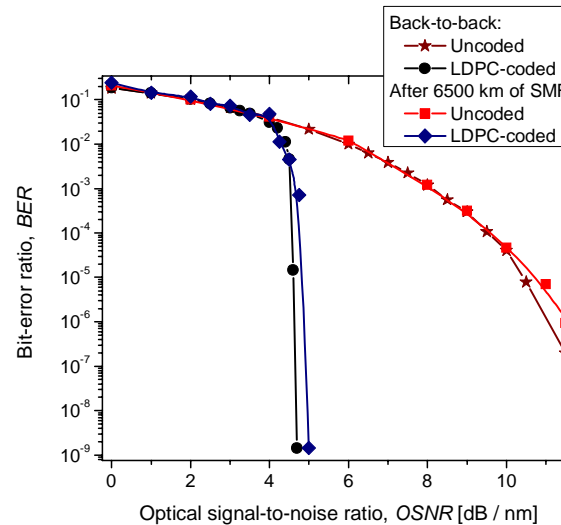


Fig. 5. BER performance of LDPC-coded OFDM system with aggregate rate of 10 Gb/s, after 6500 km of SMF.

In Fig. 6 the efficiency of LDPC-coded OFDM in simultaneous chromatic dispersion and PMD compensation is studied. After 6500 km of SMF (without optical dispersion compensation) and for DGD of 100ps, the LDPC-coded OFDM has the penalty within 1.5 dB. Notice that coded turbo equalization cannot be used at all for this level of residual chromatic

dispersion and DGD. It can also be noticed that, from numerical results presented here, that the major factor of performance degradation in LDPC-coded OFDM with direct detection, in ASE noise dominated scenario, is PMD. The main reason is that some of the subcarriers completely fade away (see [20] for the detailed explanation). To improve the tolerance to PMD someone may use longer training sequences and redistribute the transmitted information among the subcarriers less affected by DGD, or to use the polarization beam splitter and separately process x - and y -PSPs, in a fashion similar to that proposed for OFDM with coherent detection [7,12]; however, the complexity of such a scheme would be at least two times higher. Notice that for this level of DGD, the redistribution of power among subcarriers not being faded away is not needed. For larger values of DGDs, the penalty due to DGD grows as DGD increases, if the redistribution of subcarriers is not performed.

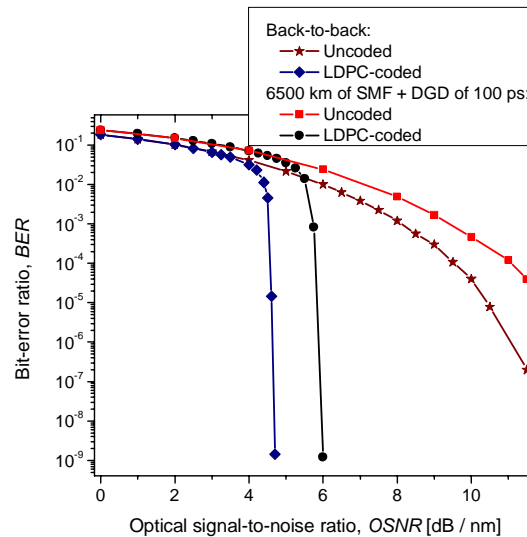


Fig. 6. BER performance of LDPC-coded OFDM system with aggregate rate of 10 Gb/s, after 6500 km of SMF and for DGD of 100 ps.

5. Conclusion

In this paper we study the LDPC-coded SSB OFDM as an efficient coded modulation scheme suitable for simultaneous chromatic dispersion and PMD compensation. We show that residual dispersion over 6500 km of SMF and DGD of 100 ps, in a system with aggregate rate 10 Gb/s, can be simultaneously compensated with penalty within 1.5 dB (with respect to the back-to-back configuration) when training sequence based channel estimation and girth-10 LDPC codes of rate 0.8 are employed. The coded-turbo equalization is not able to deal with this amount of residual chromatic dispersion and PMD if complexity of equalizer is to be kept reasonably low. We have found that in ASE noise dominated scenario, for coded-OFDM with direct detection, the degradation mostly comes from PMD. To improve the tolerance to PMD someone may either use longer training sequences to average the accumulated ASE noise in combination with redistribution of power among subcarriers not being under fading due to DGD or to use polarization-beam splitter and process x - and y -PSPs separately at the expense of increased receiver complexity. Another option would be to choose the channel coefficients by maximizing the symbol LLRs from (12).

Acknowledgments

This work was supported in part by the National Science Foundation (NSF) under Grant IHCS-0725405.